

Experimental demonstration of Quantum Overlapping Tomography

Yang Zhengning,¹ Shihao Ru,^{1,2} Lianzhen Cao,³ Nikolay Zheludev,^{1,4} and Weibo Gao^{1,4,*}

¹*Division of Physics and Applied Physics, School of Physical and Mathematical Sciences, Nanyang Technological University, Singapore 637371, Singapore*

²*School of Physics, Xi'an Jiaotong University, Xi'an 710049, China*

³*School of Physics and Photoelectric Engineering, Weifang University, Weifang 261061, China*

⁴*The Photonics Institute and Centre for Disruptive Photonic Technologies, Nanyang Technological University, Singapore 637371, Singapore*

(Dated: August 1, 2022)

Quantum tomography is one of the major challenges of large-scale quantum information research due to the exponential time complexity. In this work, we experimentally demonstrate quantum overlapping tomography [Phys. Rev. Lett. 124, 100401 (2020)], a scheme intent on characterizing critical information of a many-body quantum system in logarithmic time complexity. By comparing the measurement results of full state tomography and overlapping tomography, we show that overlapping tomography gives accurate information of the system with much fewer state measurements than full state tomography.

As more interest and effort has been put into the research of quantum information processing in recent years [1, 2], there have been remarkable advances in constructing and controlling large scale quantum systems with a series of physical systems, including but not limited to superconducting circuits [3–5], linear optics [6, 7], ion trap [8, 9], and ultracold atoms [10]. Although it has been realistic to create and operate a large system with around 100 or even 1000 qubits [11, 12], it's still a question how to measure such many-body states and to demonstrate the correlation between any two parts of the system. Due to the quantum nature of qubits, the information carried by a qubit cannot be read out with one single measurement [13]. Instead, one need to perform multiple times of measurement with multiple sets of basis on one quantum state to reconstruct the density matrix of the quantum state [14]. As the number of qubits in the system goes up, the number of required measurements increases exponentially [15], leading to an unacceptable time complexity, which could overwhelm the stability of the system for even a moderate scale. In fact, for a system with just 10 qubits, a full state tomography (FST) has been considerably hard [16]. Driven by this challenge, various protocols have been raised to reduce the time complexity. Some protocols offer advantages for certain quantum states with special structures [17]. There are also protocols that can estimate an unknown state with a higher efficiency, but they require quantum non-demolition measurement, which is still not experimentally applicable nowadays [18].

A more realistic idea is to retrieve limited but critical information by reconstructing the reduced density matrices of the small-scale subsystems of the huge-scale system, with much fewer measurements. Although this kind of ‘partial’ tomography doesn't give a full picture of the system, it is usually critical in application cases, such as the research on long-range order in many-body systems [19] and machine learning based on quantum neural net-

works [20]. However, even for this simplified task, the time complexity still can be unacceptable. Supposing we have a system of n qubits and hope to measure all the k -qubit subsystems, there are $\binom{n}{k}$ subsystems need to be measured. For small k relative to n , we have $\binom{n}{k} \sim n^k$. Thus, the time complexity is $e^{O(k)} \times n^k$ because measuring each k -qubit subsystem has a time complexity $e^{O(k)}$. Even for a modest scale of $n = 50$ and $k = 2$, the total number of measurements will reach 10000N, where N stands for the required number of measurements to obtain a statistically significant result for each measurement setting. This number has been too much for realistic experiment.

Quantum Overlapping Tomography (QOT) [21] is one protocol proposed by J. Cotler and F. Wilczek, which

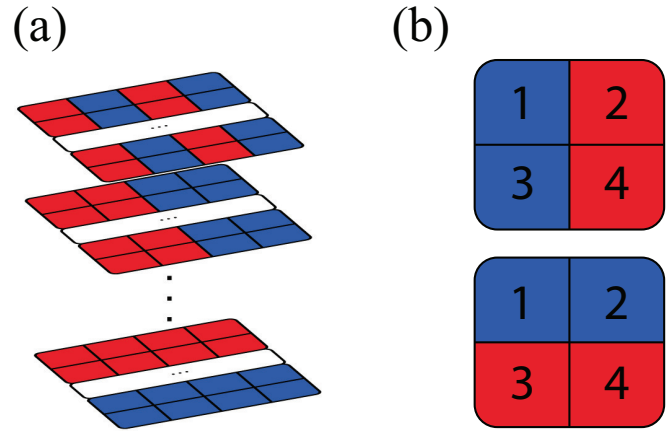


FIG. 1. (a) 2-qubit quantum overlapping tomography of a large-scale system. The whole system is divided into two groups, red and blue, in different strategies. For each dividing strategy, the two groups are measured in different basis. (b) QOT dividing strategy for $n = 4, k = 2$ case.

makes use of strong power of parallelism to simplify this task. With the overlapping nature of quantum many-body system, QOT can reconstruct all $\binom{n}{k}$ k-qubit subsystems in logarithmic time complexity $\sim e^{O(k)} \log_k n$ by reorganizing the measurement dataset. With this scheme, for $n = 50$, $k = 2$, it's possible to measure overlapped subsystems at the same time, reconstructing all the subsystems within less than 100N measurements, which means an over 100 times boost.

Due to its fascinating advantage, QOT has been attracting considerable attention from the community. Some researchers have started to use this method in their projects.[22] However, a general experimental scheme of QOT and the performance comparison between QOT and FST are still new topics to fill in. In this work, we experimentally demonstrate QOT on a 4-photon polarization entanglement system powered by spontaneous parametric down-conversion (SPDC). To apply the QOT scheme originating from exact tomography[23], which is not legitimate to use in experiment, into the experiment scenario, we develop an algorithm to perform a Bayesian mean estimation (BME)[24] to estimate the target states with the measurement dataset, for both FST and QOT. We compare the outcome of FST and QOT with a 4-photon GHZ state. To make the results comparable, the QOT estimation is performed with a subset of the measurement dataset that the FST uses, instead of a separate dataset. In addition, we generate a variation of GHZ state and

show that QOT is capable to characterize general kind of states.

In quantum information, any quantum state of a single qubit can be demonstrated with a two-dimension density matrix [23]

$$\hat{\rho} = \frac{1}{2} \sum_{i=0}^3 S_i \hat{\sigma}_i, \hat{\sigma}_0 \equiv \begin{pmatrix} 1 & 0 \\ 0 & 1 \end{pmatrix}, \hat{\sigma}_1 \equiv \begin{pmatrix} 0 & 1 \\ 1 & 0 \end{pmatrix}, \\ \hat{\sigma}_2 \equiv \begin{pmatrix} 0 & -i \\ i & 0 \end{pmatrix}, \hat{\sigma}_3 \equiv \begin{pmatrix} 1 & 0 \\ 0 & -1 \end{pmatrix} \quad (1)$$

S_i values can be given by $S_i = \text{Tr} \{ \hat{\sigma}_i \hat{\rho} \}$, which indicates that it can be directly obtained with projective measurements.

Similarly, a general multi-qubit system with n qubits can be demonstrated with a density matrix with 2^n dimensions.

$$\hat{\rho} = \frac{1}{2^n} \sum_{i_1, i_2, \dots, i_n=0}^3 S_{i_1, i_2, \dots, i_n} \hat{\sigma}_{i_1} \otimes \hat{\sigma}_{i_2} \otimes \dots \otimes \hat{\sigma}_{i_n} \quad (2)$$

To reconstruct the density matrix, the main task of a quantum full state tomography is to obtain all the S_{i_1, i_2, \dots, i_n} values. In theory, the values can be directly calculated with the results of measurement through exact tomography.[23]

$$S_{i_1, i_2, \dots, i_n} = (\lambda_1 P_{\phi_{i_1}} + \lambda_1^\perp P_{\phi_{i_1}^\perp})(\lambda_2 P_{\phi_{i_2}} + \lambda_2^\perp P_{\phi_{i_2}^\perp}) \dots (\lambda_n P_{\phi_{i_n}} + \lambda_n^\perp P_{\phi_{i_n}^\perp}) \\ = (\lambda_1 \lambda_2 \dots \lambda_n) P_{\phi_{i_1} \phi_{i_2} \dots \phi_{i_n}} + (\lambda_1 \lambda_2 \dots \lambda_n^\perp) P_{\phi_{i_1} \phi_{i_2} \dots \phi_{i_n}^\perp} + \dots + (\lambda_1^\perp \lambda_2^\perp \dots \lambda_n^\perp) P_{\phi_{i_1}^\perp \phi_{i_2}^\perp \dots \phi_{i_n}^\perp} \quad (3)$$

Here we note ϕ_{i_j} as the eigenstate with eigenvalue $\lambda_j = 1$ and $\phi_{i_j}^\perp$ with eigenvalue $\lambda_j^\perp = -1$. $P_{\phi_{i_j}^\perp}$ stands for the possibility probability. that j^{th} qubit is in $\phi_{i_j}^\perp$, which can be estimated with a finite number of measurements. For the case of $i_j = 0$, $\lambda_j P_{\phi_0} + \lambda_j^\perp P_{\phi_0^\perp} = 1$, which means this term would be “transparent” in the calculation.

For the whole system with n qubits, an array with $2n$ detectors is deployed to measure all 2^n eigenstates of element density matrix $\hat{\sigma}_{i_1} \otimes \hat{\sigma}_{i_2} \otimes \dots \otimes \hat{\sigma}_{i_n}$ at the same time, with the measurement setting $\{i_1, i_2, \dots, i_n\}$. In principle, 4^n settings are needed since each i_j has 4 possible values. However, for those settings with any $i_j = 0$, the S_{i_1, i_2, \dots, i_n} can be directly calculated with the measurement results by other settings with all $i_j = 0$. Thus, in practice we need 3^n settings to reconstruct the density matrix of a system with n qubits.

Note that exact tomography is only usable with the assumption that the observed probabilities are theoret-

ically perfect, which means the observation should be with no errors and be conducted through infinite ensemble of states. In another word, Eq(3) is not valid for any real measurement, otherwise it would lead to physically insufficient results. A common practice to reconstruct legitimate density matrices with real observation results is statistical estimation methods, such as Maximum Likelihood Estimation (MLE)[25] and Bayesian Mean Estimation (BME) [24, 26]. In this work, we develop an algorithm based on Gibbs sampling[27] to perform a Bayesian Mean Estimation with the measurement datasets for both FST and QOT.

Here we show how the QOT works in a $k = 2$ case. Firstly, we describe the task as reconstructing all $\binom{n}{k}$ 2-qubit reduced density matrices:

$$\hat{\rho}^{\{x_1, x_2\}} = \frac{1}{2^2} \sum_{i_1, i_2=0}^3 S_{i_1, i_2}^{\{x_1, x_2\}} \hat{\sigma}_{i_1} \otimes \hat{\sigma}_{i_2} \quad (4)$$

where $\{x_1, x_2\}$ represents 2-qubit subsystem of the n -qubit system. To obtain the values of $S_{i_1, i_2}^{\{x_1, x_2\}}$, Normally we need to pick all of the 2-qubit groups $\{x_1, x_2\}$ and measure them individually. For the n -qubit system, there are $\frac{n(n-1)}{2}$ of such subsystems, and $N \times 3^2 = 9N$ measurements need to be operated on each subsystem to get a tomography of them, which gives an $O(n^2)$ time complexity.

In QOT (Fig.1(a)) instead, we divide the n -qubit system into 2 groups, by $q = \lceil \log_2 n \rceil$ ways. The dividing strategy should satisfy the requirement that for any subsystem $\{x_1, x_2\}$, there is at least one divide where x_1 and x_2 are in different groups. One general strategy is that, in j^{th} divide ($j \in \{0, 1, \dots, q-1\}$),

- put all qubits x_i ($i \in \{1, 2, \dots, n\}$) in group 1 if $\lfloor \frac{i-1}{2^j} \rfloor$ gives an even number;
- put all x_i into group 2 if $\lfloor \frac{i-1}{2^j} \rfloor$ gives an odd number.

An dividing example of $n = 4$ case is given by (Fig.1(b)). The 4-qubit system, noting as $\{1, 2, 3, 4\}$, is divided in 2 different ways. In the 0^{th} divide, qubit 1 and 3 are put into group 1, qubit 2 and 4 are put into group 2; in the 1^{st} divide, qubit 1 and 2 are put into group 1, qubit 3 and 4 are put into group 2.

In principle, for each divide, we perform measurements with 3×3 settings, where all qubits in group 1(2) were measured in basis $i_1(i_2)$, $i_1, i_2 = 1, 2, 3$. But since we measure the whole system here, We can immediately notice that for the cases $i_1 = i_2 = 1, 2, 3$, the measurement settings are all same for any divide. Thus we measure the system in two steps:

1. Measure all the qubits in X,Y,Z basis respectively, which need $3N$ measurements in total.
2. For each divide out of the q divides, measure all qubits in group 1 in one basis $B_1 \in \{X, Y, Z\}$ and measure all qubits in group 2 in another different basis B_2 . Thus, it takes 6 measurements for each of the q divides, which is a total of $6qN$.

So, we use $3+6q$ measurement basis sets in total, which gives a logarithmic time complexity. With an ideal probabilities dataset, density matrices $\hat{\rho}^{\{x_1, x_2\}}$ can be reconstructed by calculating the value

$$S_{i_1, i_2}^{\{x_1, x_2\}} = (\lambda_1 P_{\phi_{i_1}} + \lambda_1^\perp P_{\phi_{i_1}^\perp})(\lambda_2 P_{\phi_{i_2}} + \lambda_2^\perp P_{\phi_{i_2}^\perp}) \quad (5)$$

This calculation relies on the same assumption as exact tomography, so it is not valid for real measurements. A proper estimation is also necessary to reconstruct legitimate density matrices with the QOT dataset.

In our experiment, we build up a 4-qubit entangled system and try to reconstruct the 2-qubit subsystems of

it. If we operate FST on the 4-qubit system, we need $N \times 3^4 = 81N$ measurements for the task. For the subsystem reconstruction task that we have discussed, $N \times \binom{4}{2} \times 3^2 = 54N$ measurements are required. However, with QOT, only $N \times (3 + 6 \log_2 4) = 15N$ measurements are required to reconstruct all the 2-qubit subsystems.

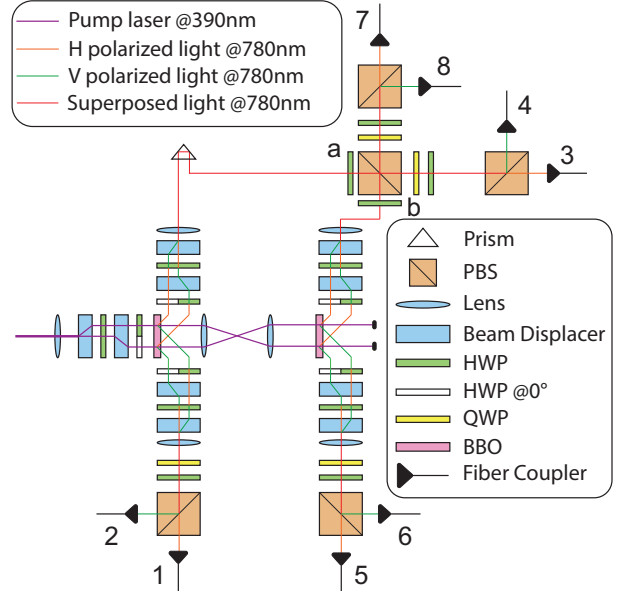


FIG. 2. Schematic of experimental set-up for generating 4-photon entanglement, with the detectors labeled by order. An ultrafast pulsed laser with the center wavelength 390nm, pulse duration ~ 100 fs and repetition rate 80MHz was deployed to pump two sets of interference-based beam-like SPDC entanglement source [28, 29]. The mass group delay dispersion of the pulsed laser caused by thick crystals is pre-compensated by 4 Brewster prisms. The polarization entangled photon pairs go through a post-selection interference to generate a 4-photon GHZ state, which is then detected and measured by 8 single-photon detectors. The PBS interference is phase insensitive, which guarantees the observed state can remain stable for days without extra phase stability control. To reduce the loss of two-fold fidelity caused by time-space correlation [30, 31], we applied narrow-band filters with $\lambda_{FWHM} = 3nm$ and $\lambda_{FWHM} = 10nm$ to the signal and idler photons respectively. The center wavelengths of both signal and idler photons are 780nm (before and after being transmitted through the narrow-band filters). BBO: Barium Borate; PBS: polarization beam-splitter; HWP: half-wave plate; QWP: quarter-wave plate

Fig.2 shows an overview of the experimental set-up for generating and detecting a 4-photon GHZ state $\psi_{GHZ}^R = \frac{1}{\sqrt{2}}(|H V H V\rangle + e^{i\theta}|V H V H\rangle)$. Following Jones Calculus [32], the horizontal polarization $|H\rangle$ and vertical polarization $|V\rangle$ are defined as the eigenstates of Pauli matrix σ_z . $|L/R\rangle = \frac{1}{\sqrt{2}}(|H\rangle \pm i|V\rangle)$, $|D/A\rangle = \frac{1}{\sqrt{2}}(|H\rangle \pm |V\rangle)$ are the eigenstates for σ_y and σ_x respectively. We use wave-plates and polarization beamsplitters to measure qubits in specific measurement basis. By detecting photons in both output modes of PBS, we measure all 16 probabili-

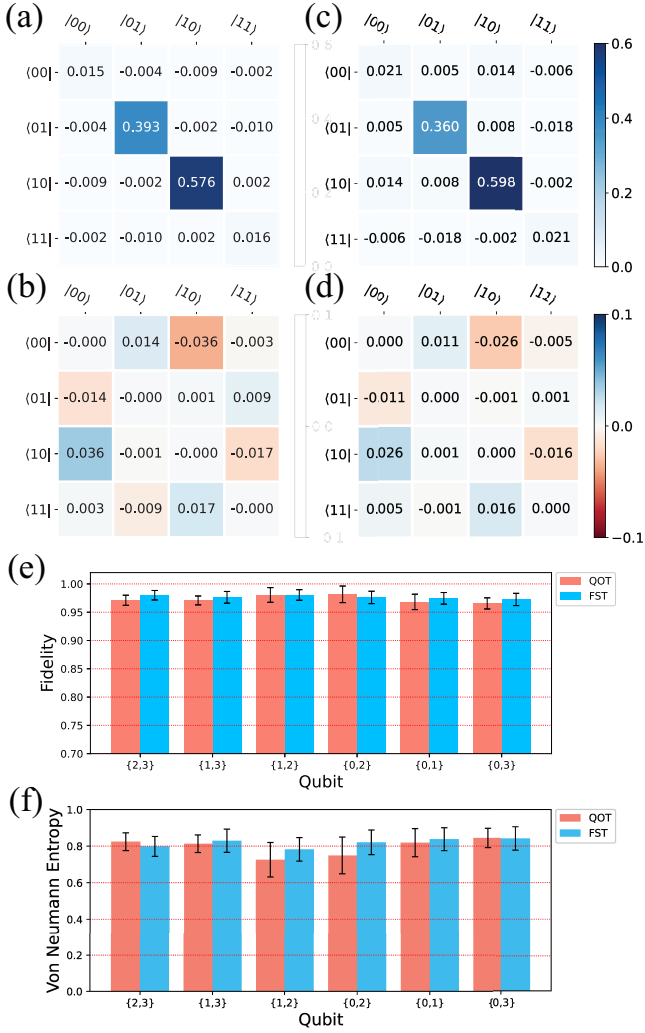


FIG. 3. (a) real and (b) imaginary part of density matrix of 2-qubit subsystem $\psi_{2,3}^F$ obtained by 4-qubit full state tomography (FST) (c) real and (d) imaginary part of density matrix of 2-qubit subsystem $\psi_{2,3}^O$ obtained by overlapping tomography. (e) 2-qubit state fidelities of $\psi_{i_1,i_2}^F/\psi_{i_1,i_2}^O$ with $(\psi_{GHZ}^R)_{i_1,i_2}$ and (f) Von Newmann Entropy of subsystem ψ_{i_1,i_2}^F and ψ_{i_1,i_2}^O . For (e-f), error bars show 95% confidence interval

ties in parallel for one measurement basis set.

The two-fold coincidence counting rate can reach 100 kHz at pump power 550 mW, with a state fidelity $F > 0.97$. The singles count rates vary between 350 - 500 kHz with different channels, generating a 2-fold accidental rate around 2 kHz and a coincidence to accidental ratio (CAR) around 50:1. The 4-fold accidental rate is around 0.05 Hz.. The single photon detecting efficiency is between 20 - 25% with narrow-band filtering. We recorded 4-fold coincidences (for 16 sets of measurement basis spontaneously) for 300 s on each setting, with the total coincidence counting rate over 16 sets of basis around 10 Hz, with a CAR around 200:1. We performed an FST on this 4-qubit state to reconstruct the 4-qubit

density matrix ρ^F . Comparing the tomography result with a given pure state $\rho^R = |\psi_{GHZ}^R\rangle\langle\psi_{GHZ}^R|$, the state fidelity $F^M = (Tr\sqrt{\sqrt{\rho^R}\rho^F\sqrt{\rho^R}})^2 = 0.922 \pm 0.013$.

For the overlapping tomography case, we focus in the 2-qubit subsystems of the 4-qubit entangled state. Thus, firstly, we obtain the density matrices of 2-qubit subsystems $\rho_{j_1,j_2}^F = Tr_{i_1,i_2}\rho^M, i_1, i_2 \in \{1, 2, 3, 4\}, \{j_1, j_2\} = \{1, 2, 3, 4\} / \{i_1, i_2\}$ by calculating the partial trace. Then we perform overlapping tomography on the same state, reconstructing the density matrices ρ_{i_1,i_2}^O of 2-qubit subsystems. By comparing ρ_{i_1,i_2}^F and ρ_{i_1,i_2}^O in density matrix visualization (Fig.3(a-d)) and state fidelity (Fig.3(e)), we confirmed that QOT gives highly similar results with the outcome from 4-qubit FST. The fidelity differences are less than 0.01 within the margin of error, which displays the similarities between density matrices estimated with QOT and 4-qubit FST.

To further characterize the states in this case, we calculated and compared the Von Neumann Entropy [33] $S = -Tr(\rho \cdot \ln \rho)$ of ρ_{i_1,i_2}^F and ρ_{i_1,i_2}^O . For the 2-qubit subsystems of an ideal 4-qubit GHZ state, the quantum state should be a mixed state consisted by two maximally entangled Bell states $|\Psi\rangle$, and the VNE should be $S \approx \ln 2 = 0.69$. State or measurement error usually increases this value, which indicates the state is more ‘mixed’ and less ‘entangled’. By comparing VNE S_{i_1,i_2}^O and S_{i_1,i_2}^F (Fig.3(f)), we find that overlapping tomography gives overall similar results with the 4-qubit FST. Though all differences between VNE results given by QOT and 4-qubit FST are within the margin of error, for some subsystems, the VNE by QOT are visibly smaller than that by FST, which seems to indicate that the QOT result is “closer” to the theoretical prediction. This may be due to the QOT results being estimated with fewer sets of measurement data than the 4-qubit FST, which rules out the influence of inconsistency of measurements originating from environment vibration and imperfect experiment operations.

Further, we use overlapping tomography to characterize an alternative state ψ' . We generated this state by setting HWP a and b in Fig.2 to $\theta_a = -22.5^\circ$ and $\theta_b = -22.5^\circ$. Similarly, we compare the result of 4-qubit FST and QOT with density matrices visualization (Fig.4(a-d)), where two methods give identical result. This result shows that the overlapping tomography is equally efficient for different multi-qubit states, indicating that QOT is a promising method to characterize common quantum states.

Based on the experimental scheme, the reference state wavefunction for this case can be written by $\psi'^R = \frac{1}{\sqrt{2}}(|D'VD''V\rangle + e^{i(\theta_1+\theta_2)}|A'HA''H\rangle)$, where $|D'\rangle = |H\rangle + e^{i\theta_1}|V\rangle, |A'\rangle = |H\rangle - e^{i\theta_1}|V\rangle, |D''\rangle = |H\rangle + e^{i\theta_2}|V\rangle, |A''\rangle = |H\rangle - e^{i\theta_2}|V\rangle$. Here, θ_1 and θ_2 are extra phases introduced by SPDC process, which can be estimated by calculating the fidelity between measure-

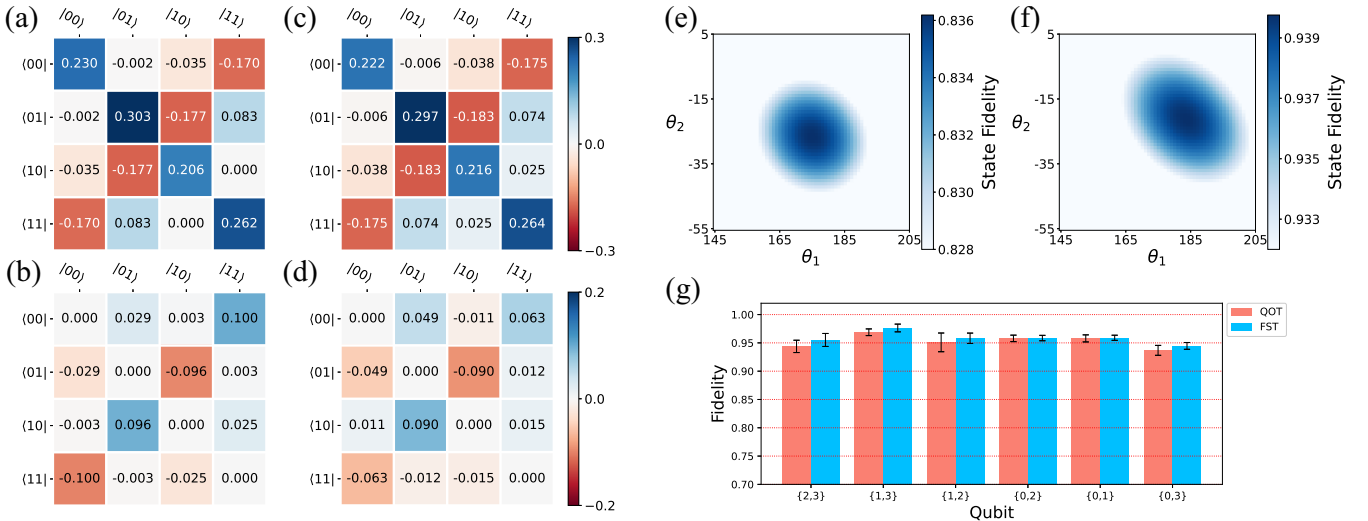


FIG. 4. (a) Real and (b) imaginary part of density matrix of 2-qubit subsystem $\psi'^F_{0,2}$ obtained by 4-qubit full state tomography (FST). (c) Real and (d) imaginary part of density matrix of 2-qubit subsystem $\psi'^O_{0,2}$ obtained by overlapping tomography. (e) State fidelity $F(\theta_1, \theta_2)$ between 4-qubit state $\psi'^F_{0,2}$ reconstructed via 4-qubit FST and reference state $\psi'^R(\theta_1, \theta_2)$, F reached peak at $\theta_1 = 175^\circ, \theta_2 = -27^\circ$. (f) State fidelity $F_{0,2}(\theta_1, \theta_2)$ between 2-qubit subsystem $\psi'^F_{0,2}$ reconstructed via overlapping tomography and reduced reference state $\psi'^R_{0,2}(\theta_1, \theta_2)$. $F_{0,2}$ reached peak at $\theta_1 = 183^\circ, \theta_2 = -21^\circ$. (g) 2-qubit state fidelity with $\psi'^R_{i_1, i_2}$ of $\psi'^F_{i_1, i_2}$ and $\psi'^O_{i_1, i_2}$, error bars show 95% confidence interval

ment result and reference states. We estimated $\theta_1 = 175^\circ, \theta_2 = -21^\circ$ by comparing the 4-qubit density matrix ρ^F obtained by 4-qubit FST with reference state $\rho'^R(\theta_1, \theta_2) = |\psi'^R(\theta_1, \theta_2)\rangle\langle\psi'^R(\theta_1, \theta_2)|$ (Fig.4(e)). We also use the subsystems reconstructed via QOT to estimate the state phase θ_1, θ_2 by comparing the density matrices $\rho'^O_{i_1, i_2}$ with reference state $\rho'^R_{i_1, i_2}(\theta_1, \theta_2)$ (Fig.4(f)). Though a visible difference exists between the two estimations, considering the small derivative of fidelity to both θ s, the results are reasonably close with each other as the difference between two estimations corresponds to less than 0.8% difference in state fidelity. Similar with the discussion over VNE results, the QOT estimation could be more reliable because there is no contribution from system inconsistency, which could be more significant when measuring systems with larger scale. This result shows that QOT can be used to extract important state parameters with a significantly reduced time complexity too. With the estimated wavefunction, we calculated and the state fidelities between the reference states and subsystems reconstructed via both 4-qubit FST and QOT (Fig.4(g)). The fidelity differences are within the margin of error as well.

In summary, we performed quantum overlapping tomography to characterize 4-qubit GHZ states. By comparing the QOT results with FST results, we showed that QOT is capable to reconstruct subsystems with a given scale and extract important parameters of a 4-qubit state, with a remarkably reduced number of measurements. This scheme is directly applicable to quantum

states with a wider range of structures and larger scale, which could be significant for the future development of quantum information.

We acknowledge Singapore National Research foundation through QEP grant (NRF2021-QEP2-01-P02, NRF2021-QEP2-03-P01, 2019-0643 (QEP-P2) and 2019-1321 (QEP-P3)) and Singapore Ministry of Education (MOE2016-T3-1-006 (S)).

* wbgao@ntu.edu.sg

- [1] T. D. Ladd, F. Jelezko, R. Laflamme, Y. Nakamura, C. Monroe, and J. L. O'Brien, Quantum computers, *Nature* **464**, 45 (2010).
- [2] M. A. Nielsen and I. Chuang, Quantum computation and quantum information (2002).
- [3] M. H. Devoret and R. J. Schoelkopf, Superconducting circuits for quantum information: an outlook, *Science* **339**, 1169 (2013).
- [4] F. Arute, K. Arya, R. Babbush, D. Bacon, J. C. Bardin, R. Barends, R. Biswas, S. Boixo, F. G. Brandao, and D. A. Buell, Quantum supremacy using a programmable superconducting processor, *Nature* **574**, 505 (2019).
- [5] Y. Wu, W.-S. Bao, S. Cao, F. Chen, M.-C. Chen, X. Chen, T.-H. Chung, H. Deng, Y. Du, and D. Fan, Strong quantum computational advantage using a superconducting quantum processor, *Physical review letters* **127**, 180501 (2021).
- [6] H.-S. Zhong, Y.-H. Deng, J. Qin, H. Wang, M.-C. Chen, L.-C. Peng, Y.-H. Luo, D. Wu, S.-Q. Gong, and H. Su, Phase-programmable gaussian boson sampling

using stimulated squeezed light, *Physical review letters* **127**, 180502 (2021).

[7] P. Kok, W. J. Munro, K. Nemoto, T. C. Ralph, J. P. Dowling, and G. J. Milburn, Linear optical quantum computing with photonic qubits, *Reviews of modern physics* **79**, 135 (2007).

[8] C. Monroe and J. Kim, Scaling the ion trap quantum processor, *Science* **339**, 1164 (2013).

[9] C. Figgatt, A. Ostrander, N. M. Linke, K. A. Landsman, D. Zhu, D. Maslov, and C. Monroe, Parallel entangling operations on a universal ion-trap quantum computer, *Nature* **572**, 368 (2019).

[10] M. Saffman, T. G. Walker, and K. Mølmer, Quantum information with rydberg atoms, *Rev. Mod. Phys.* **82**, 2313 (2010).

[11] B. Yang, H. Sun, C.-J. Huang, H.-Y. Wang, Y. Deng, H.-N. Dai, Z.-S. Yuan, and J.-W. Pan, Cooling and entangling ultracold atoms in optical lattices, *Science* **369**, 550 (2020).

[12] B. Yang, H. Sun, C.-J. Huang, H.-Y. Wang, Y. Deng, H.-N. Dai, Z.-S. Yuan, and J.-W. Pan, Cooling and entangling ultracold atoms in optical lattices, *Science* **369**, 550 (2020).

[13] K. Kraus, A. Böhm, J. Dollard, and W. Wootters, *States, effects, and operations: Fundamental notions of quantum theory* (1983).

[14] G. D'Ariano and P. L. Presti, Quantum tomography for measuring experimentally the matrix elements of an arbitrary quantum operation, *Physical review letters* **86**, 4195 (2001).

[15] R. O'Donnell and J. Wright, Efficient quantum tomography, *Proceedings of the forty-eighth annual ACM symposium on Theory of Computing*, 899 (2016).

[16] C. Song, K. Xu, W. Liu, C.-p. Yang, S.-B. Zheng, H. Deng, Q. Xie, K. Huang, Q. Guo, L. Zhang, P. Zhang, D. Xu, D. Zheng, X. Zhu, H. Wang, Y. A. Chen, C. Y. Lu, S. Han, and J.-W. Pan, 10-qubit entanglement and parallel logic operations with a superconducting circuit, *Physical Review Letters* **119**, 180511 (2017).

[17] B. P. Lanyon, C. Maier, M. Holzäpfel, T. Baumgratz, C. Hempel, P. Jurcevic, I. Dhand, A. S. Buyskikh, A. J. Daley, M. Cramer, M. B. Plenio, R. Blatt, and C. F. Roos, Efficient tomography of a quantum many-body system, *Nature Physics* **13**, 1158 (2017).

[18] S. Aaronson, Shadow tomography of quantum states, *SIAM Journal on Computing* **49**, STOC18 (2019).

[19] U. Schollwöck, The density-matrix renormalization group, *Reviews of Modern Physics* **77**, 259 (2005).

[20] M. Schuld, I. Sinayskiy, and F. Petruccione, The quest for a quantum neural network, *Quantum Information Processing* **13**, 2567 (2014).

[21] J. Cotler and F. Wilczek, Quantum overlapping tomography, *Phys. Rev. Lett.* **124**, 100401 (2020).

[22] F. B. Maciejewski, F. Baccari, Z. Zimborás, and M. Oszmaniec, Modeling and mitigation of cross-talk effects in readout noise with applications to the Quantum Approximate Optimization Algorithm, *Quantum* **5**, 464 (2021).

[23] J. Altepeter, E. Jeffrey, and P. G. Kwiat, Photonic state tomography, *Advances in Atomic Molecular and Optical Physics* **52**, 105 (2005).

[24] R. Blume-Kohout, Optimal, reliable estimation of quantum states, *New Journal of Physics* **12**, 043034 (2010).

[25] K. Banaszek, G. M. D'Ariano, M. G. A. Paris, and M. F. Sacchi, Maximum-likelihood estimation of the density matrix, *Phys. Rev. A* **61**, 010304 (1999).

[26] J. M. Lukens, K. J. H. Law, A. Jasra, and P. Lougovski, A practical and efficient approach for bayesian quantum state estimation, *New Journal of Physics* **22**, 063038 (2020).

[27] S. Geman and D. Geman, Stochastic relaxation, gibbs distributions, and the bayesian restoration of images, *IEEE Transactions on Pattern Analysis and Machine Intelligence* **PAMI-6**, 721 (1984).

[28] H.-S. Zhong, Y. Li, W. Li, L.-C. Peng, Z.-E. Su, Y. Hu, Y.-M. He, X. Ding, W. Zhang, and H. Li, 12-photon entanglement and scalable scattershot boson sampling with optimal entangled-photon pairs from parametric down-conversion, *Physical review letters* **121**, 250505 (2018).

[29] P. G. Kwiat, K. Mattle, H. Weinfurter, A. Zeilinger, A. V. Sergienko, and Y. Shih, New high-intensity source of polarization-entangled photon pairs, *Physical Review Letters* **75**, 4337 (1995).

[30] W. P. Grice, A. B. U'Ren, and I. A. Walmsley, Eliminating frequency and space-time correlations in multiphoton states, *Physical Review A* **64**, 063815 (2001).

[31] X.-L. Wang, L.-K. Chen, W. Li, H.-L. Huang, C. Liu, C. Chen, Y.-H. Luo, Z.-E. Su, D. Wu, and Z.-D. Li, Experimental ten-photon entanglement, *Physical review letters* **117**, 210502 (2016).

[32] R. C. Jones, A new calculus for the treatment of optical systems. description and discussion of the calculus, *J. Opt. Soc. Am.* **31**, 488 (1941).

[33] P. Calabrese and J. Cardy, Entanglement entropy and quantum field theory, *Journal of Statistical Mechanics: Theory and Experiment* **2004**, P06002 (2004).